applied sciences

MDPI

Article

Ag-Sensitized NIR-Emitting Yb^{3+}-Doped Glass-Ceramics

Francesco Enrichi [1,2,*], Elti Cattaruzza [2], Tiziano Finotto [2], Pietro Riello [2], Giancarlo C. Righini [3,4], Enrico Trave [2] and Alberto Vomiero [2,5]

1 CNR-ISP Istituto di Scienze Polari, c/o campus scientifico Università Ca' Foscari Venezia, via Torino 155, 30172 Mestre-Venezia, Italy
2 Dipartimento di Scienze Molecolari e Nanosistemi, Università Ca' Foscari Venezia, via Torino 155, 30172 Mestre-Venezia, Italy; cattaruz@unive.it (E.C.); tiziano@unive.it (T.F.); riellop@unive.it (P.R.); enrico.trave@unive.it (E.T.); alberto.vomiero@unive.it (A.V.)
3 Museo Storico della Fisica e Centro Studi e Ricerche "Enrico Fermi", Piazza del Viminale 1, 00184 Roma, Italy; giancarlo.righini@centrofermi.it
4 CNR-IFAC Istituto di Fisica Applicata Nello Carrara, Via Madonna del Piano 10, 50019 Sesto Fiorentino, Firenze, Italy
5 Division of Materials Science, Department of Engineering Sciences and Mathematics, Luleå University of Technology, 971 87 Luleå, Sweden
* Correspondence: francesco.enrichi@cnr.it

Received: 11 February 2020; Accepted: 14 March 2020; Published: 23 March 2020

Featured Application: downshifting layers for silicon solar cells, NIR emitting devices and lasers.

Abstract: The optical photoluminescent (PL) emission of Yb^{3+} ions in the near infrared (NIR) spectral region at about 950–1100 nm has many potential applications, from photovoltaics to lasers and visual devices. However, due to their simple energy-level structure, Yb^{3+} ions cannot directly absorb UV or visible light, putting serious limits on their use as light emitters. In this paper we describe a broadband and efficient strategy for sensitizing Yb^{3+} ions by Ag codoping, resulting in a strong 980 nm PL emission under UV and violet-blue light excitation. Yb-doped silica–zirconia–soda glass–ceramic films were synthesized by sol-gel and dip-coating, followed by annealing at 1000 °C. Ag was then introduced by ion-exchange in a molten salt bath for 1 h at 350 °C. Different post-exchange annealing temperatures for 1 h in air at 380 °C and 430 °C were compared to investigate the possibility of migration/aggregation of the metal ions. Studies of composition showed about 1–2 wt% Ag in the exchanged samples, not modified by annealing. Structural analysis reported the stabilization of cubic zirconia by Yb-doping. Optical measurements showed that, in particular for the highest annealing temperature of 430 °C, the potential improvement of the material's quality, which would increase the PL emission, is less relevant than Ag-aggregation, which decreases the sensitizers number, resulting in a net reduction of the PL intensity. However, all the Ag-exchanged samples showed a broadband Yb^{3+} sensitization by energy transfer from Ag aggregates, clearly attested by a broad photoluminescence excitation spectra after Ag-exchange, paving the way for applications in various fields, such as solar cells and NIR-emitting devices.

Keywords: sol–gel; silica–zirconia; glass–ceramics; Ag nanoaggregates; Yb^{3+} ions; energy transfer; downshifting; photoluminescence

1. Introduction

Rare earth ions (RE^{3+}) have many optical applications due to their unique spectral properties, in relation to the features of their electronic energy levels, covering UV, visible and IR [1]. This makes them excellent candidates for lighting [2–4], displays [5], biosensing [6–8], optical amplification [9], anticounterfeiting [10,11] and solar cells [12–14]. Among them, Yb^{3+} ions provide near infrared (NIR) emission around 950–1100 nm, which is interesting for many of the previously cited applications. However, the absorption and emission of Yb^{3+} ions are due to transitions between only two levels: $^2F_{7/2}$ (ground state) and $^2F_{5/2}$ (excited state). Therefore, Yb^{3+} ions are not able to directly absorb UV or visible photons, and other lanthanides are often added as codopants to provide an alternative excitation path by energy transfer, and sometimes to offer the additional possibility of photon multiplication by quantum cutting [15–19]. Nevertheless, codoping with other RE^{3+} ions still do not solve the limited excitation and absorption bandwidths and their small excitation cross sections, which are major limitations for their implementation in thin film downconverting devices and other specific applications.

In the past, silicon [20–23] or silver aggregates [24–27] were proven as broadband efficient sensitizers for Er^{3+} ions. Ag sensitization was successfully observed also for other RE^{3+} ions (Eu, Tb, Yb, Dy, Sm) [28–36]. In this paper, we will further investigate the interaction between Ag aggregates and Yb^{3+}, analyzing the role of the glass-ceramic (GC) matrix and its crystalline structure on the optical properties of the composite material. A GC is a homogeneous dispersion of ceramic nanocrystals in a glass. EXAFS studies suggest that RE^{3+} ions should be preferentially located in the nanocrystals [37], resulting in better spectroscopic properties. Additionally, zirconia has lower phonon energy and higher refractive index than silica [38]. By combining Ag enhancement with Yb^{3+}-doped silica–zirconia GC, the possibility to obtain a more efficient optical device is discussed in this paper. Compositional, structural and optical measurements were combined for retrieving information on the role and nature of Ag-aggregates controlled by $Ag^+ \leftrightarrow Na^+$ ion exchange, followed by annealing at different temperatures, and their interaction with Yb^{3+} ions for obtaining efficient sensitization and photoluminescence boosting.

2. Materials and Methods

Silica–zirconia (70%–30%) GC films were synthesized by following a sol–gel and dip-coating procedure, starting from Tetraethyl orthosilicate $Si(OC_2H_5)_4$ (TEOS) and zirconium propoxide $Zr(OC_3H_7)_4$ (ZPO) precursors, as described in [32]. As usual in sol–gel synthesis, all dopants were calculated and put in addition to this composition: 5 mol% Na was added as sodium acetate for allowing the introduction of Ag by ion exchange; 4 mol% $YbNO_3$ was added for Yb-doped samples. In short, three solutions were prepared as follows:

(1) TEOS, ethanol (EtOH), H_2O and HCl (TEOS:HCl:H_2O:EtOH = 1:0.01:2:25), adding 4 mol% $YbNO_3$ for Yb-doped samples;
(2) ZPO, acetylacetone (Acac), ethanol (ZPO:Acac:EtOH = 1:0.5:50);
(3) sodium acetate in methanol (60 mg/mL)

Solutions (1) and (2) were mixed together, then (3) was added dropwise and left stirring overnight (16 h). Multi-layer films were deposited on fused silica, with each layer annealed in air at 700 °C for 3 min. After 10 layers, 400 nm total thickness was achieved. A final annealing in air at 1000 °C for 1 h induced the crystallization of zirconia in the glass-ceramic (GC) matrix.

Undoped (label GC0) and 4 mol% Yb-doped (label GC4) films were then immersed for 1 h in a molten salt bath (1 mol% $AgNO_3$ in $NaNO_3$) at 350 °C to obtain $Ag^+ \leftrightarrow Na^+$ ion exchange (label GC0A and GC4A). Finally, post-exchange annealing in air at 380 °C (GC0B and GC4B) and 430 °C (GC0C and GC4C) were used for controlling Ag migration and aggregation [32].

The film composition was studied by Rutherford backscattering spectrometry (RBS), by 2.2 MeV $^4He^+$ beam at 160° backscattering angle in IBM geometry, and simulating the experimental spectra by the RUMP code [39]. Areal density (the natural unit of measurement for RBS) to film thickness

conversion was obtained, considering a molar density of the film equal to a weighted average between silica (2.00 g cm^{-3}) and zirconia (5.68 g cm^{-3}), according to the nominal stoichiometric composition of the matrix (70 SiO_2 – 30 ZrO_2), which was confirmed by RBS analysis.

The crystal phase identification was obtained by X-ray diffraction (XRD) at room temperature, with an X'Pert PRO diffractometer (Panalytical) using a Cu anode (Kα, λ = 1.54056 Å). Diffractograms were collected in Bragg–Brentano geometry in the 2θ range 10°–100°. Nanocrystal size was determined by Line Broadening Analysis (LBA) [40] by the Warren–Averbach method.

Photoluminescence excitation (PLE) and emission (PL) spectra were recorded by a FLS980 (Edinburgh Instruments). The excitation was provided by a xenon lamp coupled to a double-grating monochromator, while the emission from the sample was analyzed by a double-grating monochromator and recorded by a photon counting R928P (Hamamatsu) cooled at –20 °C (visible region) or by a photon counting R5509-73 (Hamamatsu) cooled at −80 °C (NIR region). The excitation wavelength for recording PL emission spectra was 330 nm, which is not absorbed by Yb^{3+} ions, while the emission wavelength for acquiring PL excitation spectra was set at 975 nm, the peak wavelength for Yb^{3+} ions $^2F_{5/2} \rightarrow {}^2F_{7/2}$ transition.

3. Results and Discussion

The film composition was confirmed by RBS analysis in agreement with the nominal values for Si, Zr and Yb. The Ag concentration depth profile (see examples in Figure 1) revealed a reduction from about 2 mol% (at surface) to 1 mol% (inner part of the film) both for the Ag-exchanged and the annealed samples. This indicates a small silver mobility in the glass ceramic matrix. Figure 1 presents the RBS spectra for the undoped samples before and after Ag-exchange, and the RUMP simulation of the latter (Figure 1a). In Figure 1b, a selected region corresponding to the Zr and Ag signals is reported, including a depth profile scale for the Zr signal, obtained from the RBS signal combined with the weighted average molar density between silica and zirconia, as described in the Experimental section. In Figure 1c, the calculated Ag depth profiling is reported for the samples GC0A, GC0B and GC0C. Post-exchange heat treatment changes only slightly the Ag profile, with no difference between sample GC0B and GC0C, within the experimental uncertainty of the RBS.

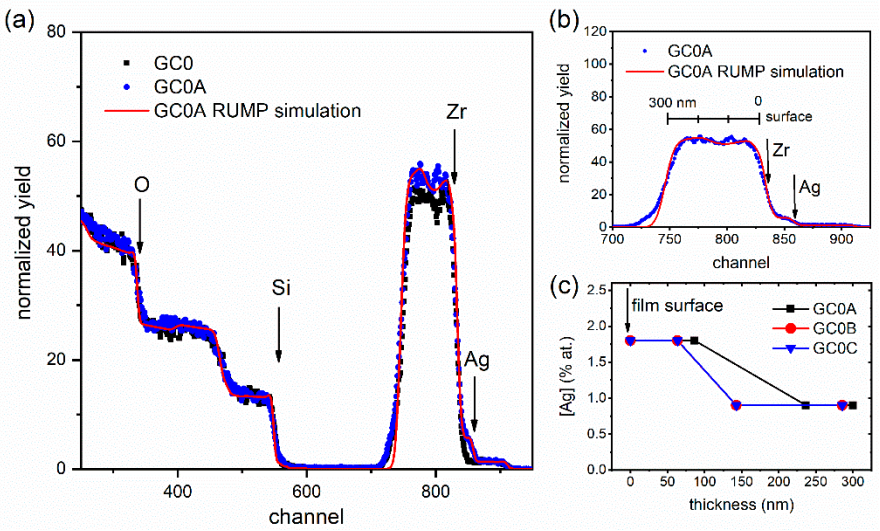

Figure 1. Full Rutherford backscattering spectrometry (RBS) spectra (**a**) and selected spectral region corresponding to Zr and Ag (**b**) for undoped samples before and after Ag-exchange (GC0 and GC0A). Ag concentration profile (**c**) as a function of film depth for samples GC0A, GC0B and GC0C. The RUMP code simulation of the GC0A spectrum is shown. In (b), the corresponding film depth is reported for the Zr signal.

XRD reflections before $Ag^+ \leftrightarrow Na^+$ ion exchange are reported in Figure 2, showing the presence of ZrO_2 tetragonal nanocrystals in the undoped samples and cubic nanocrystals in Yb-doped films, attested by a double peak (tetragonal) or a single peak (cubic) at $2\theta \approx 35.5°$ and $2\theta \approx 75°$. Noteworthy, deeper analysis which goes beyond the scope of this paper can be further exploited to corroborate the observed structural behavior and to quantify the relative phases [41]. The effect of Ag-exchange and subsequent annealing was not observed on XRD spectra. Indeed, it should be noted that crystal formation in similar materials occurs at 1000 °C. Previous studies highlighted that below that temperature, the sol-gel remains in a glassy state (see, for example, Zur et al. [19]). Ag-exchange and the following annealing processes were done at 350 °C and up to 430 °C. Therefore, it can be reasonably concluded that the energies involved at these treatment temperatures are not enough for modifying the crystalline features of the glass-ceramic material. Finally, proper line broadening analysis (LBA) of XRD diffraction peaks [40] obtained by the Warren–Averbach method showed that nanocrystal size was about 14 nm for tetragonal zirconia in our undoped samples (GC0), and about 12 nm for cubic zirconia in Yb-doped samples (GC4).

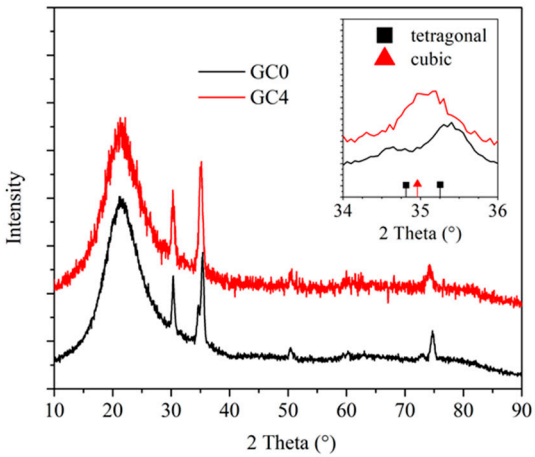

Figure 2. XRD comparison between undoped (GC0) and Yb-doped (GC4) silica-zirconia samples. The inset reports a selected region of the diffraction pattern around $2\theta \approx 35°$, attesting to different crystal structures of the two samples: tetragonal-phase (diffraction standard reference ICSD #85322) zirconia nanocrystals in undoped GC0 and cubic-phase (diffraction standard reference PDF #49-1642) zirconia nanocrystals in Yb-doped GC4.

It is known from previous studies that the optical properties of silver-doped silicate glasses have broad luminescence emissions under UV light [42–45] related to isolated Ag^+ ions (Em. 330–370 nm), Ag^+–Ag^+ pairs (Em. 430–450 nm), formation of $(Ag_3)^{2+}$ trimers, multimers, and aggregates (Em. 550–650 nm and above). Studies of the PL emission under 280 nm excitation before (GC0) and after Ag-exchange (GC0A) and 430 °C annealing (GC0C) have been reported elsewhere [32], showing a main peak at 425 nm, reasonably related to Ag+–Ag+ pairs, with a broad emission extending to the red spectral region, attributed to trimers and multimers. The modification of the curves after annealing is related to the evolution of the Ag species within the material. After annealing, the maximum peak at 425 nm slightly decreases, while the red emission contribution increases as a consequence of the decreasing of the number of dimers towards the formation of multimers and small aggregates. The optical properties of these Ag-aggregates can be better investigated by 330 nm excitation, which is reported in Figure 3. Additionally, there is also higher interest in analyzing near UV and blue excitation because sources like lasers, LEDs, or lamps for these wavelengths are much more available and cheaper than deeper UV light sources. As expected, the PL spectra of Ag-exchanged GC samples under 330 nm excitation, before (GC0A) and after annealing at 380 °C (GC0B) and 430 °C (GC0C), show a broadband emission related to multimers and aggregates, covering up to 750 nm. As previously observed [32], the intensity of this emission increases by annealing, as a possible consequence of matrix recovery with the

removal of non-radiative defects, and of the increase of the number of multimers at the expense of single ions and dimers, at least for 380 °C annealing. A further thermal treatment at 430 °C seems detrimental with respect to 380 °C annealing. The reduction of PL intensity suggests a decrease in the effective number of emitting species, which is corroborated by the following PL analysis in the NIR spectral range.

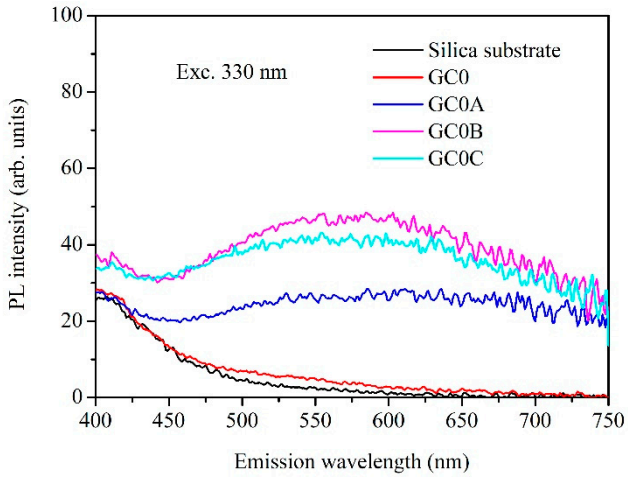

Figure 3. Photoluminescent (PL) emission by 330 nm excitation of undoped samples before Ag-exchange (GC0), after exchange (GC0A), and after annealing at 380 °C (GC0B) and 430 °C (GC0C). The broad emission, up to 750 nm and more, is reasonably attributed to Ag multimers and small aggregates.

The NIR PL emission under 330 nm excitation is reported in Figure 4b for Yb^{3+}-doped GC samples before Ag-exchange (GC4), after exchange (GC4A), and after annealing at 380 °C (GC4B) and 430 °C (GC4C). The direct excitation of Yb^{3+} ions by 330 nm light is completely absent. After Ag ion exchange, a strong Yb^{3+} PL emission peak at 975 nm is detected, possibly due to dimers, multimers or small aggregates formed during the ion exchange process, which act as efficient sensitizers. In agreement with the previous PL analysis of Ag aggregates, annealing is expected to improve the quality of the matrix, which should increase the PL intensity. However, annealing also decreases the number of sensitizers due to the formation of multimers and bigger aggregates, and this additionally increases the average distance between them and Yb^{3+} ions, reducing the efficiency of energy transfer. The overall combination of these positive and negative effects is almost balanced at 380 °C, while it results in a significant decrease in the NIR PL signal at 430 °C. Therefore, Ag as-exchanged samples are actually the best performing NIR emitters.

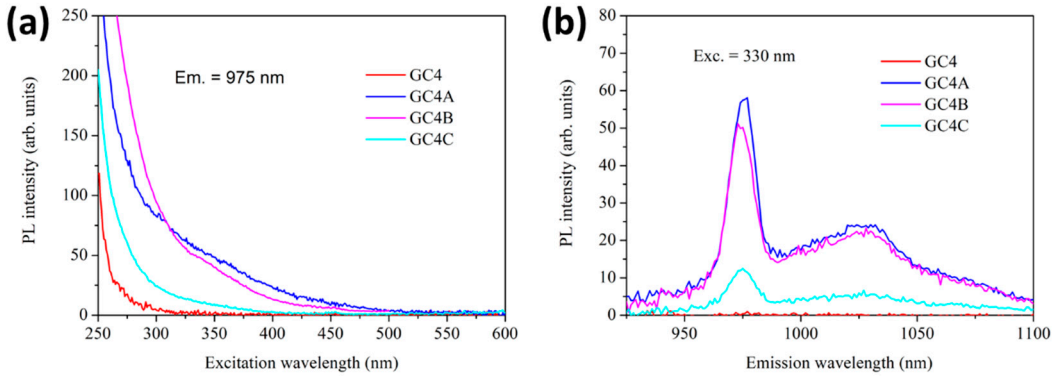

Figure 4. PL excitation (**a**) and near-infrared (NIR) emission (**b**) of Yb-doped samples before Ag-exchange (GC4), after exchange (GC4A), and after annealing at 380 °C (GC4B) and 430 °C (GC4C). A broadband excitation up to about 500 nm can be observed after Ag-exchange. Moreover, 330 nm wavelength is not absorbed by Yb^{3+} ions, while it provides a strong PL emission in Ag-exchanged samples.

Deeper investigation of the excitation behavior of Yb^{3+}-doped GC samples, before and after Ag-exchange and annealing, is reported in Figure 4a. The intensity of the PLE curves agrees well with the PL analysis described above, with a further remarkable feature: the possibility for efficient and broadband excitation on Ag-exchanged samples, covering the whole spectral range from UV to blue, up to about 500 nm. On the contrary, the PLE spectrum of Yb^{3+}-doped samples before Ag-exchange (GC4) gives no signal above 300 nm excitation. Below that wavelength, the possible excitation of Yb^{3+} ions is due to the occurrence of charge-transfer processes from the matrix itself.

4. Conclusions

The synthesis and characterization of efficient NIR emitting glass-ceramic films is presented and discussed. Yb^{3+}-doped silica-zirconia-soda materials are prepared by sol-gel and dip-coating. Annealing in air at 1000 °C induces the precipitation of zirconia nanocrystals. Different crystalline phases have been observed, depending on the presence of the RE dopant: tetragonal for undoped, and cubic for Yb^{3+}-doped glass-ceramics. The following $Ag^{+} \leftrightarrow Na^{+}$ ion exchange allows the introduction of Ag species as dimers, multimers, and aggregates in the film, which can be excited in the UV spectral region, and act as sensitizers for Yb^{3+} ions. As a consequence, Yb^{3+} NIR emission around 950–1100 nm is significantly enhanced after Ag ion exchange, not only in intensity, but also in the broadness of the excitation band, covering spectral regions not allowed for the direct absorption of Yb^{3+} ions. Ag-sensitized Yb^{3+}-doped films could have applications as spectral downshifters for photovoltaic (PV) solar cells and NIR light-emitting sources. Furthermore, the high versatility and optical quality of sol-gel glass-ceramic waveguides make these materials also suitable for realizing solar concentrators and integrated optical devices, such as optical amplifiers and lasers.

Author Contributions: Conceptualization by F.E.; data acquisition and analysis by F.E., E.C., T.F., P.R., E.T., A.V.; resources by F.E., E.C., P.R., G.C.R., E.T., A.V.; writing by F.E.; funding acquisition by F.E., G.C.R., A.V. All authors have read and agreed to the published version of the manuscript.

Funding: The research was partially supported by Centro Fermi through the MiFo project and the Italy-South Africa PLESC bilateral project (Ministero Affari Esteri e Coop. Internazionale, MAECI). F.E. acknowledges VINNOVA for support through the Nano2Solar project (Vinnmer Marie Curie Incoming, Ref. N. 2016-02011), and A.V. acknowledges the Knut & Alice Wallenberg Foundation and the Kempe Foundation, the European Union's Horizon 2020 R&I (grant agreement N. 654002), and INFN-LNL, Legnaro, Italy for RBS analyses.

Conflicts of Interest: The authors declare no conflicts of interest.

References

1. *Spectroscopic Properties of Rare Earths in Optical Materials*; Liu, G.; Jacquier, B. (Eds.) Springer-Verlag: Berlin, Germany, 2006; ISBN 978-3-540-28209-9.
2. Jia, X.; Puthen-Veettil, B.; Xia, H.; Yang, T.C.J.; Lin, Z.; Zhang, T.; Wu, L.; Nomoto, K.; Conibeer, G.; Perez-Wurfl, I. All-silicon tandem solar cells: Practical limits for energy conversion and possible routes for improvement. *J. Appl. Phys.* **2016**, *119*, 233102. [CrossRef]
3. Lin, Y.C.; Karlsson, M.; Bettinelli, M. Inorganic phosphor materials for lighting. *Top. Curr. Chem.* **2016**, *374*, 1–47. [CrossRef]
4. Marin, R.; Sponchia, G.; Riello, P.; Sulcis, R.; Enrichi, F. Photoluminescence properties of YAG:Ce 3+,Pr 3+ phosphors synthesized via the Pechini method for white LEDs. *J. Nanoparticle Res.* **2012**, *14*. [CrossRef]
5. Kim, C.H.; Kwon, I.E.; Park, C.H.; Hwang, Y.J.; Bae, H.S.; Yu, B.Y.; Pyun, C.H.; Hong, G.Y. Phosphors for plasma display panels. *J. Alloys Compd.* **2000**, *311*, 33–39. [CrossRef]
6. Liu, Y.; Tu, D.; Zhu, H.; Chen, X. Lanthanide-doped luminescent nanoprobes: Controlled synthesis, optical spectroscopy, and bioapplications. *Chem. Soc. Rev.* **2013**, *42*, 6924–6958. [CrossRef] [PubMed]
7. Enrichi, F.; Riccò, R.; Meneghello, A.; Pierobon, R.; Cretaio, E.; Marinello, F.; Schiavuta, P.; Parma, A.; Riello, P.; Benedetti, A. Investigation of luminescent dye-doped or rare-earth-doped monodisperse silica nanospheres for DNA microarray labelling. *Opt. Mater. (Amst.)* **2010**, *32*. [CrossRef]
8. Enrichi, F. Luminescent amino-functionalized or erbium-doped silica spheres for biological applications. *Annals of the New York Academy of Sciences* **2008**, *1130*, 262–266. [CrossRef] [PubMed]

9. Desurvire, E. *Erbium-Doped Fiber Amplifiers: Principles and Applications*; John Wiley & Sons Inc.: New York, NY, USA, 1994; ISBN 0471589772.
10. Moretti, E.; Pizzol, G.; Fantin, M.; Enrichi, F.; Scopece, P.; Nuñez, N.O.; Ocaña, M.; Benedetti, A.; Polizzi, S. Deposition of silica protected luminescent layers of Eu:$GdVO_4$ nanoparticles assisted by atmospheric pressure plasma jet. *Thin Solid Films* **2016**, *598*. [CrossRef]
11. Moretti, E.; Pizzol, G.; Fantin, M.; Enrichi, F.; Scopece, P.; Ocaña, M.; Polizzi, S. Luminescent Eu-doped $GdVO_4$ nanocrystals as optical markers for anti-counterfeiting purposes. *Chem. Pap.* **2017**, *71*. [CrossRef]
12. Chiappini, A.; Zur, L.; Enrichi, F.; Boulard, B.; Lukowiak, A.; Righini, G.C.; Ferrari, M. Glass ceramics for frequency conversion. In *Solar Cells and Light Management: Materials, Strategies and Sustainability*; Enrichi, F., Righini, G.C., Eds.; Elsevier: Amsterdam, The Netherlands, 2019; ISBN 9780081027622.
13. Trupke, T.; Green, M.A.; Würfel, P. Improving solar cell efficiencies by down-conversion of high-energy photons. *J. Appl. Phys.* **2002**, *92*, 1668–1674. [CrossRef]
14. Richards, B.S. Enhancing the performance of silicon solar cells via the application of passive luminescence conversion layers. *Sol. Energy Mater. Sol. Cells* **2006**, *90*, 2329–2337. [CrossRef]
15. Enrichi, F.; Armellini, C.; Belmokhtar, S.; Bouajaj, A.; Chiappini, A.; Ferrari, M.; Quandt, A.; Righini, G.C.; Vomiero, A.; Zur, L. Visible to NIR downconversion process in Tb3+-Yb3+codoped silica-hafnia glass and glass-ceramic sol-gel waveguides for solar cells. *J. Lumin.* **2018**, *193*, 44–50. [CrossRef]
16. Bouajaj, A.; Belmokhtar, S.; Britel, M.R.; Armellini, C.; Boulard, B.; Belluomo, F.; Di Stefano, A.; Polizzi, S.; Lukowiak, A.; Ferrari, M.; et al. Tb^{3+}/Yb^{3+} codoped silica-hafnia glass and glass-ceramic waveguides to improve the efficiency of photovoltaic solar cells. *Opt. Mater. (Amst.)* **2016**, *52*. [CrossRef]
17. Lakshminarayana, G.; Qiu, J. Near-infrared quantum cutting in RE3+/Yb3+ (RE = Pr, Tb, and Tm): GeO2-B2O3-ZnO-LaF3 glasses via downconversion. *J. Alloys Compd.* **2009**, *481*, 582–589. [CrossRef]
18. Katayama, Y.; Tanabe, S. Downconversion for 1μm luminescence in lanthanide and Yb3+-codoped phosphors. In *Solar Cells and Light Management: Materials, Strategies and Sustainability*; Enrichi, F., Righini, G.C., Eds.; Elsevier: Amsterdam, The Netherlands, 2019; ISBN 9780081027622.
19. Zur, L.; Armellini, C.; Belmokhtar, S.; Bouajaj, A.; Cattaruzza, E.; Chiappini, A.; Coccetti, F.; Ferrari, M.; Gonella, F.; Righini, G.C.; et al. Comparison between glass and glass-ceramic silica-hafnia matrices on the down-conversion efficiency of Tb3+/Yb3+ rare earth ions. *Opt. Mater. (Amst.)* **2019**, *87*, 102–106. [CrossRef]
20. Falconieri, M.; Borsella, E.; De Dominicis, L.; Enrichi, F.; Franzò, G.; Priolo, F.; Iacona, F.; Gourbilleau, F.; Rizk, R. Study of the Si-nanocluster to Er3+ energy transfer dynamics using a double-pulse experiment. *Opt. Mater. (Amst.)* **2006**, *28*. [CrossRef]
21. Gourbilleau, F.; Dufour, C.; Levalois, M.; Vicens, J.; Rizk, R.; Sada, C.; Enrichi, F.; Battaglin, G. Room-temperature 1.54 μm photoluminescence from Er-doped Si-rich silica layers obtained by reactive magnetron sputtering. *J. Appl. Phys.* **2003**, *94*. [CrossRef]
22. Enrichi, F.; Mattei, G.; Sada, C.; Trave, E.; Pacifici, D.; Franzò, G.; Priolo, F.; Iacona, F.; Prassas, M.; Falconieri, M.; et al. Study of the energy transfer mechanism in different glasses co-doped with Si nanoaggregates and Er^{3+} ions. *Opt. Mater. (Amst.)* **2005**, *27*. [CrossRef]
23. Enrichi, F.; Mattel, G.; Sada, C.; Trave, E.; Pacific, D.; Franzò, G.; Priolo, F.; Iacona, F.; Prassas, M.; Falconieri, M.; et al. Evidence of energy transfer in an aluminosilicate glass codoped with Si nanoaggregates and Er^{3+} ions. *J. Appl. Phys.* **2004**, *96*. [CrossRef]
24. Trave, E.; Back, M.; Cattaruzza, E.; Gonella, F.; Enrichi, F.; Cesca, T.; Kalinic, B.; Scian, C.; Bello, V.; Maurizio, C.; et al. Control of silver clustering for broadband Er3+luminescence sensitization in Er and Ag co-implanted silica. *J. Lumin.* **2018**, *197*, 104–111. [CrossRef]
25. Martucci, A.; De Nuntis, M.; Ribaudo, A.; Guglielmi, M.; Padovani, S.; Enrichi, F.; Mattei, G.; Mazzoldi, P.; Sada, C.; Trave, E.; et al. Silver-sensitized erbium-doped ion-exchanged sol-gel waveguides. *Appl. Phys. A Mater. Sci. Process.* **2005**, *80*. [CrossRef]
26. Strohhöfer, C.; Polman, A. Silver as a sensitizer for erbium. *Appl. Phys. Lett.* **2002**, *81*. [CrossRef]
27. Mazzoldi, P.; Padovani, S.; Enrichi, F.; Mattei, G.; Sada, C.; Trave, E.; Guglielmi, M.; Martucci, A.; Battaglin, G.; Cattaruzza, E.; et al. Sensitizing effects in Ag-Er co-doped glasses for optical amplification. In Proceedings of the SPIE—The International Society for Optical Engineering, Volume 5451, Photonics Europe, Strasbourg, France, 18 August 2004.

28. Ye, S.; Guo, Z.; Wang, H.; Li, S.; Liu, T.; Wang, D. Evolution of Ag species and molecular-like Ag cluster sensitized Eu3+emission in oxyfluoride glass for tunable light emitting. *J. Alloys Compd.* **2016**, *685*, 891–895. [CrossRef]
29. Jiménez, J.A.; Lysenko, S.; Liu, H.; Fachini, E.; Cabrera, C.R. Investigation of the influence of silver and tin on the luminescence of trivalent europium ions in glass. *J. Lumin.* **2010**, *130*, 163–167. [CrossRef]
30. Abbass, A.E.; Swart, H.C.; Kroon, R.E. Effect of silver ions on the energy transfer from host defects to Tb ions in sol-gel silica glass. *J. Lumin.* **2015**, *160*, 22–26. [CrossRef]
31. Li, J.; Wei, R.; Liu, X.; Guo, H. Enhanced luminescence via energy transfer from Agˆ+ to RE ions (Dyˆ3+, Smˆ3+, Tbˆ3+) in glasses. *Opt. Express* **2012**, *20*, 10122–10127. [CrossRef]
32. Enrichi, F.; Cattaruzza, E.; Ferrari, M.; Gonella, F.; Ottini, R.; Riello, P.; Righini, G.C.; Trave, E.; Vomiero, A.; Zur, L. Ag-Sensitized Yb3+ Emission in Glass-Ceramics. *Micromachines* **2018**, *9*, 380. [CrossRef]
33. Enrichi, F.; Belmokhtar, S.; Benedetti, A.; Bouajaj, A.; Cattaruzza, E.; Coccetti, F.; Colusso, E.; Ferrari, M.; Ghamgosar, P.; Gonella, F.; et al. Ag nanoaggregates as efficient broadband sensitizers for Tb3+ ions in silica-zirconia ion-exchanged sol-gel glasses and glass-ceramics. *Opt. Mater. (Amst.)* **2018**, *84*, 668–674. [CrossRef]
34. Lin, H.; Chen, D.; Yu, Y.; Zhang, R.; Wang, Y. Molecular-like Ag clusters sensitized near-infrared down-conversion luminescence in oxyfluoride glasses for broadband spectral modification. *Appl. Phys. Lett.* **2013**, *103*. [CrossRef]
35. Enrichi, F.; Armellini, C.; Battaglin, G.; Belluomo, F.; Belmokhtar, S.; Bouajaj, A.; Cattaruzza, E.; Ferrari, M.; Gonella, F.; Lukowiak, A.; et al. Silver doping of silica-hafnia waveguides containing Tb^{3+}/Yb^{3+} rare earths for downconversion in PV solar cells. *Opt. Mater. (Amst.)* **2016**, *60*.
36. Enrichi, F.; Cattaruzza, E.; Ferrari, M.; Gonella, F.; Martucci, A.; Ottini, R.; Riello, P.; Righini, G.C.; Trave, E.; Vomiero, A.; et al. Role of Ag multimers as broadband sensitizers in Tb3+/Yb3+ co-doped glass-ceramics. *SPIE Proceedings. Fiber Lasers Glas. Photonics Mater. Appl.* **2018**, *10683*.
37. Afify, N.D.; Dalba, G.; Rocca, F. XRD and EXAFS studies on the structure of Er3+-doped SiO 2-HfO2 glass-ceramic waveguides: Er3+-activated HfO2 nanocrystals. *J. Phys. D Appl. Phys.* **2009**, *42*, 115416. [CrossRef]
38. Zhao, X.; Vanderbilt, D. Phonons and lattice dielectric properties of zirconia. *Phys. Rev. B—Condens. Matter Mater. Phys.* **2002**, *65*, 075105. [CrossRef]
39. Doolittle, L.R. Algorithms for the rapid simulation of Rutherford backscattering spectra. *Nucl. Instrum. Methods Phys. Res. Sect. B Beam Interact. Mater. Atoms.* **1985**, *9*, 344–351. [CrossRef]
40. Enzo, S.; Polizzi, S.; Benedetti, A. Applications of fitting techniques to the Warren-Averbach method for X-ray line broadening analysis. *Zeitschrift fur Krist.—New Cryst. Struct.* **1985**, *170*, 275–287.
41. Wiemer, C.; Lamperti, A.; Lamagna, L.; Salicio, O.; Molle, A.; Fanciulli, M. Detection of the Tetragonal Phase in Atomic Layer Deposited La-Doped ZrO2 Thin Films on Germanium. *J. Electrochem. Soc.* **2011**, *158*, G194. [CrossRef]
42. Cattaruzza, E.; Caselli, V.M.; Mardegan, M.; Gonella, F.; Bottaro, G.; Quaranta, A.; Valotto, G.; Enrichi, F. Ag+↔Na+ion exchanged silicate glasses for solar cells covering: Down-shifting properties. *Ceram. Int.* **2015**, *41*, 7221–7226. [CrossRef]
43. Cattaruzza, E.; Mardegan, M.; Trave, E.; Battaglin, G.; Calvelli, P.; Enrichi, F.; Gonella, F. Modifications in silver-doped silicate glasses induced by ns laser beams. *Appl. Surf. Sci.* **2011**, *257*, 5434–5438. [CrossRef]
44. Borsella, E.; Battaglin, G.; Garcìa, M.A.; Gonella, F.; Mazzoldi, P.; Polloni, R.; Quaranta, A. Structural incorporation of silver in soda-lime glass by the ion-exchange process: A photoluminescence spectroscopy study. *Appl. Phys. A* **2000**, *132*, 125–132.
45. Borsella, E.; Gonella, F.; Mazzoldi, P.; Quaranta, A.; Battaglin, G.; Polloni, R. Spectroscopic investigation of silver in soda-lime glass. *Chem. Phys. Lett.* **1998**, *284*, 429–434. [CrossRef]